Inorg. Chem. **2004**, *43*, 7691–7701

Aqueous Speciation Studies of Europium(III) Phosphotungstate

Cheng Zhang, Robertha C. Howell, Kymora B. Scotland, Frances G. Perez, Louis Todaro, and Lynn C. Francesconi*

Department of Chemistry, Hunter College and Graduate School of the City University of New York, New York, New York 10021

Received March 15, 2004

The incorporation of lanthanide ions into polyoxometalates may be a unique approach to generate new luminescent, magnetic, and catalytic functional materials. To realize these new applications of lanthanide polyoxometalates, it is imperative to understand the solution speciation chemistry and its impact on solid-state materials. In this study we find that the aqueous speciation of europium(III) and the trivacant polyoxometalate, $PW_9O_{34}^{9-}$, is a function of pH, countercation, and stoichiometry. For example, at low pH, the lacunary $(PW_{11}O_{39})^{7-}$ predominates and the 1:1 $Eu(PW_{11}O_{39})^{4-}$, **2**, forms. As the pH is increased, the 1:2 complex, $Eu(PW_{11}O_{39})_2^{11-}$ species, **3**, and $(NH_4)_{22}\{(Eu_2PW_{10}O_{38})_4(W_3O_8(H_2O)_2(OH)_4\}\cdot 44H_2O$, a Eu_8 hydroxo/oxo cluster, **1**, form. Countercations modulate this effect; large countercations, such as K^+ and Cs^+, promote the formation of species **3** and **1**. Addition of Al(III) as a counterion results in low pH and formation of $\{Eu(H_2O)_3(\alpha\text{-}2\text{-}P_2W_{17}O_{61})\}_2$, **4**, with Al(III) counterions bound to terminal W–O bonds. The four species observed in these speciation studies have been isolated, crystallized, and characterized by X-ray crystallography, solution multinuclear NMR spectroscopy, and other appropriate techniques. These species are **1**, $(NH_4)_{22}\{(Eu_2PW_{10}O_{38})_4(W_3O_8(H_2O)_2(OH)_4\}\cdot 44H_2O$ ($P\bar{1}$; $a = 20.2000(0)$, $b = 22.6951(6)$, $c = 25.3200(7)$ Å; $\alpha = 65.6760(10)$, $\beta = 88.5240(10)$, $\gamma = 86.0369(10)°$; $V = 10550.0(5)$ Å^3; $Z = 2$), **2**, $Al(H_3O)\{Eu(H_2O)_2PW_{11}O_{34}\}\cdot 20H_2O$ ($P\bar{1}$, $a = 11.4280(23)$, $b = 11.5930(23)$, $c = 19.754(4)$ Å; $\alpha = 103.66(3)$, $\beta = 95.29(3)$, $\gamma = 102.31(3)°$; $V = 2456.4(9)$ Å^3; $Z = 2$), **3**, $Cs_{11}Eu(PW_{11}O_{34})_2\cdot 28H_2O$ ($P\bar{1}$; $a = 12.8663(14)$, $b = 19.8235(22)$, $c = 21.7060(23)$ Å; $\alpha = 114.57(0)$, $\beta = 91.86(0)$, $\gamma = 102.91(0)°$; $V = 4858.3(9)$ Å^3; $Z = 2$), **4**, $Al_2(H_3O)_8\{Eu(H_2O)_3(\alpha\text{-}2\text{-}P_2W_{17}O_{61})\}_2\cdot 29H_2O$ ($P\bar{1}$; $a = 12.649(6)$, $b = 16.230(8)$, $c = 21.518(9)$ Å; $\alpha = 111.223(16)$, $\beta = 94.182(18)$, $\gamma = 107.581(17)°$; $V = 3842(3)$ Å^3; $Z = 1$).

Introduction

Polyoxometalates (POMs) containing Keggin and Wells–Dawson moieties are chemically robust, easily modified with respect to incorporation of transition metal ions, charge, size, and potential, and can be rendered soluble in water or organic solution. Due to these features, POMs have been developed as catalysts for oxidation and acid-dependent reactions.

Lanthanide (Ln) ions can offer unique functionality when combined with polyoxometalates. We envision that incorporation of Ln ions into POMs offers unique functionality, for example, in the creation of luminescent,[1] magnetic, and Lewis acid catalytic centers.[2] In the area of developing novel functional materials, lanthanide ions, by means of their multiple coordination numbers, can link polyoxometalates into solid-state oligomers[3,4] and large wheel structures.[5–8] POMs can serve as connectors and transfer agents for different monolacunary POMs.[9]

While solid-state crystal structures show the numerous possibilities for use of lanthanide ions in forming new polyoxometalate families, understanding the solution speciation chemistry and its impact on the solid-state chemistry is critical to define new applications. Such an understanding of the complex solution speciation and dynamics for POMs, in general, and Ln POMs, specifically, is lacking. Polyoxometalate composition in aqueous solution is dynamic; multiequilibria exist depending on pH, countercation, concentration, and aging of the solution. Lanthanide ions also show complex dynamic behavior in aqueous solution.

We and others have studied the aqueous chemistry of lanthanide complexes of the monovacant lacunary polyoxometalates, specifically, $(\alpha_2\text{-}P_2W_{17}O_{61})^{10-}$ and $(\alpha_1\text{-}P_2W_{17}O_{61})^{10-}$ isomers, where the lanthanide ion is incorporated into the

* Author to whom correspondence should be addressed. E-mail: lfrances@hunter.cuny.edu.

10.1021/ic049655h CCC: $27.50
Published on Web 10/28/2004

"cap" and "belt" regions of the POM, respectively.[3,4,10−16] A number of species exist in solution and in the solid state, and focused solution speciation studies coupled with crystallography provide insight into the chemistry and stabilities of the solution species.

The trivacant polyoxotungstate, $XW_9O_{34}^{n-}$, has the potential to support lanthanide clusters. $XW_9O_{34}^{n-}$ is derived from the Keggin structure (X = P, n = 9; X = Si, n = 10; X = As(V), n = 9), and this anion has six oxygen atoms available for bonding (in the Aα form) and seven (in the Bα form). We isolated a unique Ln_8 cluster tied together by $PW_9O_{34}^{9-}$ under neutral to basic conditions.[17] This species is very stable in water at pH 6.5−9. Examination of the solution chemistry of Eu(III) and $PW_9O_{34}^{9-}$ revealed interesting and complex behavior of lanthanide phosphotungstates that is reported herein.

The objective of this work is to examine the speciation of lanthanide complexes of $PW_9O_{34}^{9-}$ as a function of solution conditions. To this end, we studied the variations of Eu(III) and $PW_9O_{34}^{9-}$ with respect to pH, countercation, and stoichiometry, parameters that are well-known to influence POM and Ln POM speciation. We employ Eu(III) in these studies because the shift properties allow convenient monitoring by ^{31}P NMR.

To unambiguously assign the species, we optimized reaction conditions of Eu(III) and $PW_9O_{34}^{9-}$ to isolate the four compounds that are observed in the speciation studies. These compounds were characterized by appropriate solution and solid-state techniques, including multinuclear NMR and X-ray crystallography. The solid-state crystal structures not only are consistent with the solution species but also reveal the unique abilities of the countercations to influence speciation and structure.

Experimental Section

General Methods. All reagents were commercially available and used without further purification. Nanopure water was obtained from a Millipore Reverse Osmosis Direct-Q System. Elemental analyses were carried out by inductive coupled plasma atomic emission spectrometry (ICP-AES, SECTROFLAME M120E) as described below. IR spectra were recorded on a Perkin-Elmer 1625 FT-IR at room temperature from KBr pellets. Sodium 9-tungstophosphate (Na_9A-$PW_9O_{34}\cdot 16H_2O$) was prepared according to a published method[18] and identified by infrared spectroscopy.

Reaction Chemistry. Reaction of the Polyoxometalate A-α-$PW_9O_{34}^{9-}$ as a Function of Countercation and pH. Method i. Buffer solutions of LiOAc (0.5M), NaOAc (0.5 M), KOAc (0.5 M), and CsOAc (0.5 M) were each prepared at pH 4.75 (30% D_2O). Na_9A-$PW_9O_{34}^{9-}$ (sodium salt) (0.1 g) was added with vigorous stirring into four vials each containing 3 mL of buffer.

Method ii. A 3 mL volume of A-$PW_9O_{34}^{9-}$ (sodium salt) (0.1 g) aqueous solution (30% D_2O) was prepared at pH 1, 3, 5, 7.3, 8, and 10.35 by using HCl or NaOH to adjust the pH. The solutions from both methods i and ii were heated to 90 °C for 2 min. The solutions were cooled to room temperature and then placed into 10 mm NMR tubes. The ^{31}P NMR spectra were recorded, and the data are listed in Table S1 (Supporting Information).

Reaction of A-$PW_9O_{34}^{9-}$ with Eu^{3+} (1:1 Stoichiometry) as a Function of pH Monitored by ^{31}P NMR. A 0.056 mmol amount of Eu^{3+} (50 μL of 1.12 M) was added into four vials each containing 3 mL of H_2O (30% D_2O), respectively; A-PW_9 (0.1527 g, 0.056

(1) Key references to lanthanide luminescence: (a) Bunzli, J.-C. G. Luminescent Probes. In *Lanthanide Probes in Chemistry, Biology and Earth Sciences*; Bunzli, J.-C. G., Choppin, G., Eds.; Elsevier: Amsterdam, 1989. (b) Kido, J.; Okamoto, Y. *Chem. Rev.* **2002**, *102*, 2357−2368. (c) Bruce, J. I.; Dickins, R. S.; Govenlock, L. J.; Gunnlaugsson, T.; Lopinski, S.; Lowe, M. P.; Parker, D.; Peacock, R. D.; Perry, J. J. B.; Aime, S.; Botta, M. *J. Am. Chem. Soc.* **2000**, *122*, 9674−9684. (d) Dickins, R. S.; Aime, S.; Batsanov, A. S.; Beeby, A.; Botta, M.; Bruce, J. I.; Howard, J. A. K.; Love, C. S.; Parker, D.; Peacock, R. D.; Puschmann, H. *J. Am. Chem. Soc.* **2002**, *124*, 12697−12705. (e) Parker, D.; Dickins, R. S.; Puschmann, H.; Crossland, C.; Howard, J. A. K. *Chem. Rev.* **2002**, *102*, 1977−2010. Key reviews on new functional materials, particularly electrochromic, electroluminescent, photochromic, and photoluminescent materials: (f) Katsoulis, D. E. *Chem. Rev.* **1998**, *98*, 359−387. (g) Yamase, T. *Chem. Rev.*, **1998**, *98*, 307−325. Recent applications of lanthanide polyoxometalates incorporated into materials follow. Electrochromic device preparation: (h) Liu, S.; Kurth, D. G.; Mohwald, H.; Volkmer, D. *Adv. Mater.* **2002**, *14*, 225−228. Photoluminescent films: (i) Mo, Y.-G.; Dillon, R. O.; Snyder, P. G.; Tiwald, T. E. *Thin Solid Films* **1999**, *355*−*356*, 1−5. (j) Xu, L.; Zhang, H.; Wang, E.; Kurth, D. G.; Li, Z. *J. Mater. Chem.* **2002**, *12*, 654−657. (k) Xu, L.; Zhang, H.; Wang, E.; Wu, A.; Li, Z. *Mater. Chem. Phys.* **2002**, *77*, 484−488. (l) Wang, Y.; Wang, X.; Hu, C.; Shi, C. *J. Mater. Chem.* **2002**, *12*, 703−707. (m) Wang, J.; Liu, F.; Fu, L.; Zhang, H. *Mater. Lett.* **2002**, *56*, 300−304. (n) Wang, Y.; Wang, X.; Hu, C. *J. Colloid Interface Sci.* **2002**, *249*, 307−315. (o) Wang, J.; Wang, H. S.; Fu, L. S.; Liu, F. Y.; Zhang, H. J. *Thin Solid Films* **2002**, *414*, 256−261.

(2) Key references to lanthanide Lewis acid catalysis: (a) Aspinall, H. C. *Chem. Rev.* **2002**, *102*, 1807−1850. (b) Molander, G. A. *Chemtracts: Org. Chem.* **1998**, *11*, 237−263. (c) Molander, G. *Chem. Rev.* **1992**, *92*, 29−68. (d) Shibasaki, M.; Yoshikawa, N. *Chem. Rev.* **2002**, *102*, 2187−2209. (e) Kobayashi, S.; Kawamura, M. *J. Am. Chem. Soc.* **1998**, *120*, 5840−5841. (f) Kobayashi, S. *Pure Appl. Chem.* **1998**, *70*, 1019−1026. (g) Aspinall, H. C.; Dwyer, J. L. M.; Greeves, N.; McIver, E. G.; Woolley, J. C. *Organometallics* **1998**, *17*, 1884−1888. (h) Xie, W.-H.; Yu, L.; Chen, D.; Li, J.; Ramirez, J.; Miranda, N. F.; Wang, P. G. In *Environmentally Benign Chemistry: Green Chemistry*; Anastas, P. T., Williamson, T. C., Eds.; Oxford University Press: Oxford, U.K., 1998; pp 129−149.

(3) Sadakane, M.; Dickman, M. H.; Pope, M. T. *Angew. Chem., Int. Ed.* **2000**, *39*, 2914−2916.

(4) Mialane, P.; Lisnard, L.; Mallard, A.; Marrot, J.; Antic-Fidancev, E.; Aschehoug, P.; Vivien, D.; Secheresse, F. *Inorg. Chem.* **2003**, *42*, 2102−2108.

(5) Muller, A.; Peters, F.; Pope, M. T.; Gatteschi, D. *Chem. Rev.* **1998**, *98*, 239−271.

(6) Muller, A.; Krickemeyer, E.; Bogge, H.; Schmidtmann, M.; Peters, F. *Angew. Chem., Int. Ed.* **1998**, *37*, 3360−3365.

(7) Muller, A.; Sarkar, S.; Shah, S. Q. N.; Bogge, H.; Schmidtmann, M.; Sarker, S.; Kogerler, P.; Hauptfleish, B.; Trautwein, A. X.; Schunemann, V. *Angew. Chem., Int. Ed.* **1999**, *38*, 3238−3241.

(8) Wassermann, K.; Dickman, M. H.; Pope, M. T. *Angew. Chem., Int. Ed. Engl.* **1997**, *36*, 1445−1448.

(9) Belai, N.; Sadakane, M.; Pope, M. T. *J. Am. Chem. Soc.* **2001**, *123*, 2087−2088.

(10) Bartis, J.; Dankova, M.; Blumenstein, M.; Francesconi, L. C. *J. Alloys Compd.* **1997**, *249*, 56−68.

(11) Bartis, J.; Sukal, S.; Dankova, M.; Kraft, E.; Kronzon, R.; Blumenstein, M.; Francesconi, L. C. *J. Chem. Soc., Dalton Trans.* **1997**, 1937−1944.

(12) Bartis, J.; Dankova, M.; Lessmann, J. J.; Luo, Q.-H.; Horrocks, W. D., Jr.; Francesconi, L. C. *Inorg. Chem.* **1999**, *38*, 1042−1053.

(13) Luo, Q.; Howell, R. C.; Dankova, M.; Bartis, J.; Williams, C. W.; Horrocks, W. D., Jr.; Young, J., V. G.; Rheingold, A. L.; Francesconi, L. C.; Antonio, M. R. *Inorg. Chem.* **2001**, *40*, 1894−1901.

(14) Luo, Q.; Howell, R. C.; Bartis, J.; Dankova, M.; Horrocks, W. D., Jr.; Rheingold, A. L.; Francesconi, L. C. *Inorg. Chem.* **2002**, *41*, 6112−6117.

(15) Sadakane, M.; Dickman, M. H.; Pope, M. T. *Inorg. Chem.* **2001**, *40*, 2715−2719.

(16) Sadakane, M.; Ostuni, A.; Pope, M. T. *J. Chem. Soc., Dalton Trans.* **2002**, 63−67.

(17) Howell, R. C.; Perez, F. G.; Jain, S.; Horrocks, W. D., Jr.; Rheingold, A. L.; Francesconi, L. C. *Angew. Chem., Int. Ed.* **2001**, *40*, 4301−4304.

(18) Domaille, P. J. *Inorg. Synth.* **1990**, *27*, 100−101.

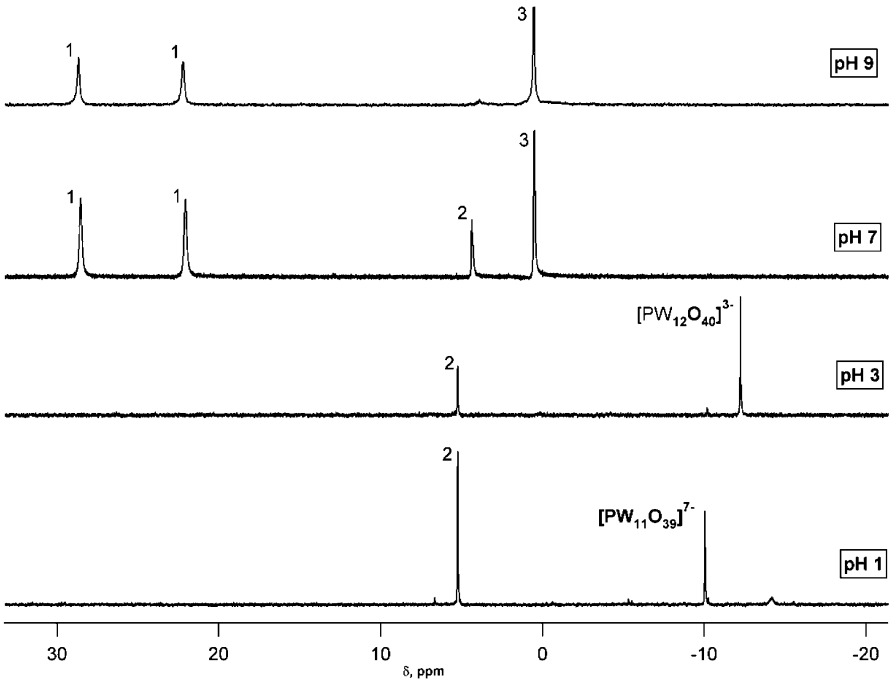

Figure 1. ^{31}P NMR spectra for reactions of $PW_9O_{34}^{9-}$ + Eu^{3+} (1:1 stoichiometry) as a function of pH. The numbers represent the species, see text, that give rise to the designated ^{31}P NMR resonances.

mmol) was added slowly to the above solutions with vigorous stirring, and the pH of resulting solutions were adjusted to 1, 3, 7, and 9 by adding diluted HCl or NaOH, followed by heating to 90 °C for 2 min. The solutions were cooled to room temperature and then placed into 10 mm NMR tubes. The ^{31}P NMR spectrum was recorded and is shown in Figure 1. The pH did not change significantly during the NMR measurement.

A-$PW_9O_{34}^{9-}$ with Eu^{3+} (1:1 Stoichiometry) as a Function of Countercation and pH. Buffer solutions of LiOAc (0.5 M), NaOAc (0.5 M), and KOAc (0.5 M) were prepared at three pH values (4.5, 5.5, 6.5) (30% D_2O). Preparation of solutions: 0.056 mmol Eu^{3+} (50 μL of 1.12 M) was added into nine vials each containing 3 mL of buffer. A-$PW_9O_{34}^{9-}$ (0.1527 g, 0.056 mmol) was added slowly with vigorous stirring to obtain slightly cloudy solutions that were heated at 90 °C for 2 min to form clear solutions. The solutions were cooled to room temperature and then placed into 10 mm NMR tubes. The ^{31}P NMR spectra were recorded and are shown in Figures S1 and S2 (Supporting Information).

Expanded Study of A-$PW_9O_{34}^{9-}$ with Eu^{3+} (1:1 Stoichiometry) as a Function of Countercation, including Cs^+ and Al(III). A 0.056 mmol amount of Eu^{3+} (50 μL of 1.12 M) was added into four vials containing 3 mL of H_2O (30% D_2O). A-$PW_9O_{34}^{9-}$ (0.1527 g, 0.056 mmol) was added slowly to the above solutions with vigorous stirring; the resulting solutions were heated to 90 °C for 2 min. NaCl (0.990 g, 0.56 M), KCl (0.125 g, 0.56 M), CsCl (0.113 g, 0.22 M), and $AlCl_3$ (0.135 g, 0.19 M) were added to each of the vials during the heating stage. The vials were cooled to room temperature, and the pH of the solutions was measured and found in all cases except Al(III) to be ca. 7; for Al(III), the pH was 2−3. The solutions were placed into 10 mm NMR tubes. The ^{31}P NMR spectra were recorded, and the spectra are shown in Figure 2. The pH after the experiment did not change significantly.

Reaction of A-$PW_9O_{34}^{9-}$ with Eu^{3+} as a Function of Organic Countercations, Tetrabutylammonium (TBA) Bromide and Tetraethylammonium (TEA) Bromide. (The following reaction performed in 1:1 or 2:1 Eu:A-$PW_9O_{34}^{9-}$ stoichiometry yields the same product.) To $EuCl_3 \cdot 6H_2O$ (0.32 g, 0.87 mmol) dissolved in H_2O (25 mL) was added $Na_9PW_9O_{34} \cdot 15H_2O$ (2.44 g, 0.87 mmol) to form a cloudy solution. After heating at 90 °C for 10 min, cooling and filtering off a small amount of insoluble material, tetrabutylammonium bromide (2.78 g, 8.7 mmol) was added to form a white precipitate. This crude precipitate can be collected by filtration. Further purification can be achieved by extracting three times with CH_2Cl_2 (50 mL). The organic layer was collected and the solvent evaporated and dried under vacuum.

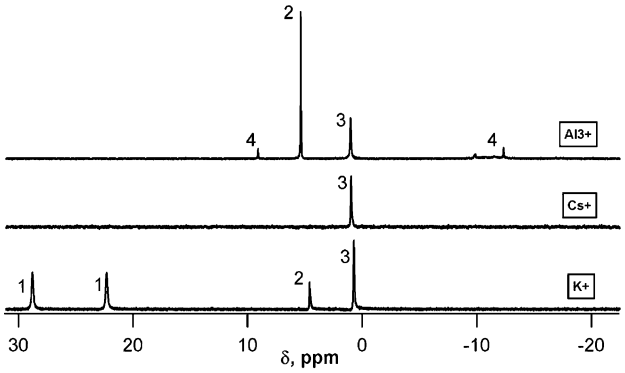

Figure 2. ^{31}P NMR spectra of reactions of $PW_9O_{34}^{9-}$ + Eu^{3+} (1:1 stoichiometry) with different countercations (see text for concentrations of countercations, pH 7, except for Al(III), where the pH 2−3). The numbers represent the species, see text, that give rise to the designated ^{31}P NMR resonances.

Reaction of A-$PW_9O_{34}^{9-}$ with Eu^{3+} as a Function of Stoichiometry (Eu:A-$PW_9O_{34}^{9-}$ = 0.5:1, 1:1, 2:1). The reaction of Eu^{3+} and A-$PW_9O_{34}^{9-}$ in 2:1, 1:1, and 0.5:1 ratios was carried out in buffer solution NaOAc (0.5 M, pH 6.5). A 50 μL (0.056 mmol) volume of 1.12 M Eu^{3+} each was added into three vials containing 3 mL of NaOAc (0.5 M, pH 6.5) (30% D_2O). Amounts of 0.3054 g (0.112 mmol), 0.1527 g (0.056 mmol), and 0.07635 g (0.028 mmol) of A-PW_9 were added slowly to the above solutions with vigorous stirring. The resulting solutions were heated to 90 °C for 2 min, followed by cooling to room temperature. The ^{31}P NMR

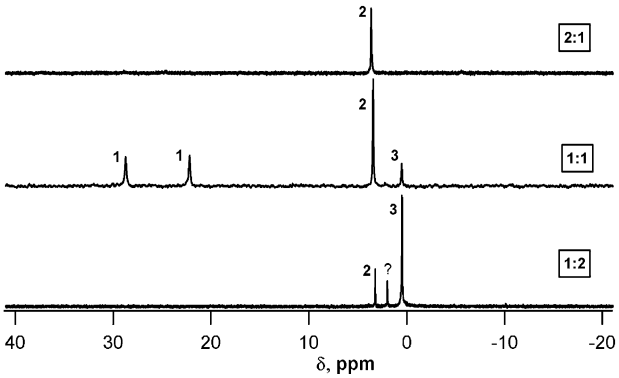

Figure 3. ^{31}P NMR spectra of reactions of $PW_9O_{34}^{9-} + Eu^{3+}$ as a function of stoichiometry. The boxed ratios represent the stoichiometric ratio of Eu:POM; therefore, the bottom spectrum represents the 1:2 Eu:$PW_9O_{34}^{9-}$ stoichiometry, the middle spectrum represents the 1:1 Eu:$PW_9O_{34}^{9-}$ stoichiometry, and the top spectrum represents 2:1 Eu:$PW_9O_{34}^{9-}$ stoichiometry. The solution species are indicated by the numbers above the resonances; see text.

spectrum is shown in Figure 3. When the experiment was carried out in water, not NaOAc buffer, the same results are obtained with a few more unidentified peaks for the 1:2 Eu:$PW_9O_{34}^{9-}$ combination (not shown).

Preparation and Crystallization of the Individual Species That Are Observed in Speciation Experiments. The syntheses of complexes **1**−**4** from Eu(III) and A-$PW_9O_{34}^{9-}$ were optimized, and the complexes were isolated and characterized by X-ray crystallography, elemental analysis, infrared spectroscopy, and multinuclear NMR.

Preparation and Crystallization of $(NH_4)_{22}\{(Eu_2PW_{10}O_{38})_4(W_3O_8(H_2O)_2(OH)_4\}\cdot 44H_2O$, 1. 1 was prepared by a modification of the procedure reported previously.[17] Solid $Na_9A\text{-}PW_9O_{34}\cdot 16H_2O$ (4.90 g, 1.8 mmol) was added slowly to a solution of $EuCl_3\cdot 6H_2O$ (0.66 g, 1.8 mmol) in 15 mL of H_2O. The resulting cloudy solution was heated to about 80 °C, and within a few seconds, a clear solution formed. Solid NH_4Cl (5.16 g, 54 mmol) was added to the hot solution, a white precipitate was formed immediately, and the solution was heated for an additional 5 min. The resulting solution turned clear and then was cooled in an ice bath. The crystallized solid was collected by filtration and recrystallized from hot water. Yield: 2.78 g, 76%. X-ray-quality crystals were obtained at 4 °C by recrystallizing 1 g of the white crystalline solid from 8 mL of hot water. Anal. Calcd for $(NH_4)_{22}\{Eu_2PW_{10}O_{38})_4(W_3O_8(H_2O)_2(OH)_4\}\cdot 44H_2O$: W, 60.11; Eu, 9.25; P, 0.94. Found: W, 60.10; Eu, 9.30; P, 0.88. IR (KBr, cm^{-1}) (metal−oxygen stretching region): 1092 (m), 1055 (m), 1025 (m), 951 (s), 935 (s), 820 (vs), 790 (s).

Preparation and Crystallization of $Al(H_3O)\{Eu(H_2O)_2PW_{11}O_{34}\}\cdot 20H_2O$, 2. To a solution of $EuCl_3\cdot 6H_2O$ (0.66 g, 1.8 mmol) in 15 mL of H_2O was added $Na_9A\text{-}PW_9O_{34}\cdot 16H_2O$ (2.45 g, 0.9 mmol) slowly with vigorous stirring to form a slightly cloudy solution. Heating at 80 °C and addition of $AlCl_3$ (1.74 g, 7.2 mmol) resulted in a clear solution. Stirring at room temperature was continued for 20 min. Traces of a precipitate were removed by filtration. The solution was stored in a beaker and allowed to slowly evaporate. After 1 week, needlelike crystals were obtained. Yield: 1.2 g, 45%. X-ray-quality crystals were selected from the bulk crystals and cut into 0.1 × 0.12 × 0.25 mm^3 blocks. Anal. Calcd for $Al(H_3O)\{Eu(H_2O)_2PW_{11}O_{34}\}\cdot 20H_2O$: W, 61.51; Eu, 4.62; P, 0.94; Al, 0.82. Found: W, 61.59; Eu, 4.67; P, 0.95; Al, 0.88. IR (KBr, cm^{-1}) (metal−oxygen stretching region): 1093 (m), 1051 (m), 957(s), 833 (s).

Preparation and Crystallization of $Cs_{11}Eu(PW_{11}O_{34})_2\cdot 28H_2O$, 3. Solid $Na_9A\text{-}PW_9O_{34}\cdot 16H_2O$ (2.45 g, 0.9 mmol) was added slowly to a solution of $EuCl_3\cdot 6H_2O$ (0.33 g, 0.9 mmol) in 7.5 mL of H_2O to obtain a slightly cloudy solution. Heating to 80 °C resulted in a clear solution within a few minutes. Solid CsCl (2.27 g, 13.5 mmol) was added to the hot solution resulting immediately in the formation of a white precipitate. Heating was continued for an additional 5 min, and then the resulting slurry was cooled in an ice bath. The solid was collected by filtration. Yield: 1.86 g, 82%. X-ray-quality crystals were obtained by recrystallizing 0.5 g of the white solid from 6 mL of warm water (50 °C). Anal. Calcd for $Cs_{11}Eu(PW_{11}O_{34})_2\cdot 28H_2O$: W, 53.02; Eu, 1.99; P, 0.81. Found: W, 53.64; Eu, 2.13; P, 0.81. IR (KBr, cm^{-1}) (metal−oxygen stretching region): 1084 (m), 1056 (m), 1023 (m), 943 (s), 776 (s).

Preparation and Crystallization of $Al_2(H_3O)_8\{Eu(H_2O)_3(\alpha\text{-}2\text{-}P_2W_{17}O_{61})\}_2\cdot 29H_2O$, 4. Solid $Na_9A\text{-}PW_9O_{34}\cdot 16H_2O$ (2.45 g, 0.9 mmol) was added slowly to a solution of $EuCl_3\cdot 6H_2O$ (0.33 g, 0.9 mmol) in 7.5 mL of H_2O to form a cloudy solution. Heating to 80 °C resulted in a clear solution within seconds. Solid $AlCl_3$ (4.34 g, 18 mmol) was added, and the resulting clear solution was heated for an additional 3 min. Traces of a precipitate were removed by filtration. The solution was stored in a vial at room temperature. After 1 month, small thick rectangular-like crystals were grown, and X-ray-quality crystals were selected from the bulk crystals. Yield: 0.7 g, 53%. Anal. Calcd for $Al_2(H_3O)_8\{Eu(H_2O)_3(\alpha\text{-}2\text{-}P_2W_{17}O_{61})\}_2\cdot 29H_2O$: W, 65.84; Eu, 3.20; P, 1.31; Al, 0.57. Found: W, 64.71; Eu, 3.21; P, 1.10; Al, 0.56. IR (KBr, cm^{-1}) (metal−oxygen stretching region): 1100 (m), 1046 (m), 954 (vs), 893 (m), 820 (s), 773 (vs), 722 (s).

Analytical Techniques. Elemental Analysis by ICP. (i) Standard Solution Preparation. The standard solution of P (0.2, 0.4, 0.6, 0.8, 1.2 ppm), Eu (1, 2, 4, 6 ppm), W (20, 40, 60, 80, 120 ppm), Al (0.5, 1, 1.5, 2.5 ppm), Na (1, 3, 5, 7 ppm), and K (1, 3, 5, 7 ppm) was prepared by diluting 1000 ppm ICP standard solution (GFS Chemicals, Inc.) with distilled water.

(ii) Sample Preparation. Crystals of complex **1**−**4** were collected by filtration, air-dried, and then further dried in a desiccator over $CaSO_4$, under vacuum for 1.5 h. The samples were left in the closed desiccator overnight. Afterward, 0.0508 g of **1**, 0.0470 g of **2**, 0.0526 g of **3**, and 0.0510 g of **4** were each dissolved in 50 mL of distilled water. The 1 and 2 mL solutions from each stock solution were diluted to 25 mL with water and used for ICP measurements.

(iii) Measurement Method. The maximum wavelength for different element was selected (P, 213.618 nm; Eu, 381.970 nm; W, 239.709 nm; Al, 308.215 nm; Na, 589.592 nm; K, 766.496 nm). A calibration curve for each element was constructed. After the calibration curve of each element was completed, the concentrations (in ppm) were determined for the two solutions of each sample (40.64, 81.28 μg/mL of **1**; 37.60, 75.20 μg/mL of **2**; 42.08, 84.16 μg/mL of **3**; 40.80, 81.60 μg/mL of **4**). The concentrations, in ppm, were converted to weight percent of each element.

Collection of NMR Data. All NMR spectra were recorded on a JEOL GX-400 spectrometer with 5 or 10 mm tubes. Resonance frequencies are 161.8 MHz for ^{31}P and 16.7 for ^{183}W. Chemical shifts are given with respect to external 85% H_3PO_4 for ^{31}P and 2.0 M Na_2WO_4 for ^{183}W. Typical acquisition parameters for ^{31}P spectra included the following: spectral width, 10 000 Hz; acquisition time, 0.8 s; pulse delay, 1 s; pulse width, 15 μs (50° tip angle). From 200 to 1000 scans were required. Generally, the 1 s pulse delay was sufficient for accurate integration of the ^{31}P peaks and, thus, qualitative assessment of concentrations of species could be

Table 1. Crystal and Structure Refinement Data for Species **1**−**4**

	1	**2**	**3**	**4**
empirical formula	$Eu_8O_{228}P_4W_{43}$	$AlEuO_{41}PW_{11}$	$ClCs_{11}EuKO_{93}P_2W_{22}$	$K_2Al_4Eu_2O_{168}P_4W_{34}$
fw	12 893.11	2888.26	7283.16	9552.82
cryst syst	triclinic	triclinic	triclinic	triclinic
space group	$P\bar{1}$ (No. 2)	$P\bar{1}$ (No. 2)	$P\bar{1}$ (No. 2)	$P\bar{1}$ (No. 2)
temp, K	109(2)	100(2)	100(2)	100(2)
wavelength, Å	0.710 73	0.710 73	0.710 73	0.710 73
a, Å	20.2000(0)	11.4280(23)	12.8663(14)	12.649(6)
b, Å	22.6951(6)	11.5930(23)	19.8235(22)	16.230(8)
c, Å	25.3200(7)	19.754 (4)	21.7060(23)	21.518(9)
α, deg	65.6760(10)	103.66(3)	114.57(0)	111.223(16)
β, deg	88.5240(10)	95.29(3)	91.86(0)	94.182(18)
γ, deg	86.0360(10)	102.31(3)	102.91(0)	107.581(17)
V, Å^3	10 550.0 (5)	2456.4(9)	4858.3(9)	3842(3)
Z	2	2	2	1
calcd density, g/cm^3	4.058	3.905	4.979	4.129
abs coeff, mm^{-1}	25.816	27.029	30.832	26.373
F(000)	11 140	2466	6212	4136
θ range, deg	1.77−27.50	1.89−27.45	1.04−28.40	1.04−28.74
limiting indices	$-26 \le h \le 26$ $-29 \le k \le 29$ $-32 \le l \le 32$	$-14 \le h \le 14$ $-14 \le k \le 15$ $-25 \le l \le 25$	$-16 \le h \le 16$ $-26 \le k \le 22$ $0 \le l \le 28$	$-14 \le h \le 16$ $-21 \le k \le 13$ $-27 \le l \le 28$
reflcns collcd/unique	141 901/48 396 [*R*(int) = 0.0386]	21 306/11 183 [*R*(int) = 0.0286]	18 777/18 777 [*R*(int) = 0.0000]	27 206/16 035 [*R*(int) = 0.0500]
refinement meth	full-matrix least squares on F^2	full-matrix least squares on F^2	full-matrix least squares on F^2	full-matrix least squares on F^2
data/restraints/params	48 396/0/1408	11 183/0/491	18 777/0/705	16 035/0/519
GOF on F^2	1.071	1.096	0.986	1.055
final R indices [$I > 2\sigma(I)$]	R1 = 0.0534, wR2 = 0.1292	R1 = 0.0572, wR2 = 0.1624	R1 = 0.0818, wR2 = 0.2135	R1 = 0.0778, wR2 = 0.2158
R indices (all data)	R1 = 0.0624, wR2 = 0.1347	R1 = 0.0687, wR2 = 0.1770	R1 = 0.1170, wR2 = 0.2391	R1 = 0.0946, wR2 = 0.2293
largest diff peak and hole, e Å^{-3}	5.373 and −4.87	11.94 and −3.807	8.071 and −7.938	9.386 and −8.749

made. For ^{183}W spectra, typical conditions included the following: spectral width, 10 000 Hz; acquisition time, 1.6 s; pulse delay, 0.5 s; pulse width, 50 μs (45° tip angle). From 1000 to 30 000 scans were acquired. For all spectra, the temperature was controlled to ±0.2 deg. For both ^{31}P and ^{183}W chemical shifts, the convention used is that the more negative chemical shifts denote more upfield resonances.

Single-Crystal X-ray Structure Determination. Crystals of **1**−**4** were examined under a thin layer of mineral oil using a polarizing microscope. Selected crystals were mounted on a glass fiber and quickly placed in a stream cold nitrogen on a Bruker SMART CCD diffractometer equipped with a sealed tube Mo anode (Kα radiation, λ = 0.710 73 Å) and graphite monochromator or Nonius Kappa CCD diffractometer. The data were collected at around 100 K. Data collection, indexing, and initial cell refinements were all handled using SHELXTL software. The SHELX package of software was used to solve and refine the restructures.[19] The heaviest atoms were located by direct methods, and the remaining atoms were found in subsequent Fourier difference syntheses. For the ammonium salt **1**, the data did not support discrimination between oxygen and nitrogen atoms. All refinements were full-squares on F^2. Crystal data and structure refinement parameters for **1**−**4** are listed in Table 1. Selected bond distances for **1**−**4** are given in Table 2. Final atomic coordinates and displacement parameters of **1**−**4** are given in the Supporting Information.

Results

Solution Chemistry. Solution Speciation of $PW_9O_{34}^{9-}$. A-$PW_9O_{34}^{9-}$ is formed from Na_2WO_4 and H_3PO_4 at pH 9.[20,21] Hill and co-workers examined the fundamental stability of A- and B-$PW_9O_{34}^{9-}$ under buffered neutral (physiological pH 7.4) aqueous media by ^{31}P NMR spectroscopy and found that, at equilibrium conditions, predominantly the monolacunary α-$PW_{11}O_{39}^{7-}$ species formed in the presence of two buffers (sulfite and tris).[22] Also, unidentified phosphorus-containing products were formed that were buffer dependent. In this study, we examined the solution behavior of the A-$PW_9O_{34}^{9-}$, at equilibrium, under different pH (1−10) and countercation (Li^+, Na^+, K^+, Cs^+, Al^{3+}) conditions by ^{31}P NMR (Supporting Information Table S1). In acidic solution the major species formed are H_3PO_4, the Keggin anion $PW_{12}O_{40}^{3-}$, and the monolacunary Keggin anion, $PW_{11}O_{39}^{7-}$. In buffer (0.5 M, LiOAc, NaOAc, KOAc) at pH 4.75, only two species H_3PO_4 and $PW_{11}O_{39}^{7-}$ exist in the solution. Under neutral conditions, $PW_{11}O_{39}^{7-}$ along with PO_4^{3-} and unidentified species were present, similar to the previous study.[22] In basic solutions, the major species formed are PO_4^{3-} and WO_4^{2-} (according to ^{183}W NMR data), consistent with decomposition of the A-$PW_9O_{34}^{9-}$. The addition of the Al^{3+} to the solution of A-$PW_9O_{34}^{9-}$ results in a lowering of the pH to about 2−3 and the observation of two equal-intensity peaks at −10.7 and −11.45 ppm that may indicate a Wells−Dawson anion, for example, the *β*-Wells−Dawson anion or an Al(III) adduct of the α-$P_2W_{18}O_{62}^{6-}$ or possibly incorporation of the Al(III) into α2-$P_2W_{17}O_{61}^{10-}$. These two peaks were in small concentration (13%); the majority of

(19) Sheldrick, G. M. *SHELXTL*; Brucker AXS, Inc., Bruker Advanced X-ray Solutions: Madison, WI, 1999.
(20) Contant, R. *Inorg. Synth.* **1990**, *27*, 71.
(21) Contant, R.; Herve, G. *Rev. Inorg. Chem.* **2002**, *22*, 63−111.
(22) Hill, C. L.; Weeks, M. S.; Schinazi, R. F. *J. Med. Chem.* **1990**, *33*, 2767−2772.

Table 2. Selected Bond Lengths (Å) for Species **1**−**4**

		Compound **1**			
Eu(1)−O(1)	2.436(10)	Eu(3)−O(1)	2.396(13)	Eu(3)−O(16B)	2.377(13)
Eu(1)−O(13)	2.346(11)	Eu(3)−O(15)	2.479(11)	Eu(3)−O(19B)	2.451(11)
Eu(2)−O(13)	2.391(13)	Eu(3)−O(16)	2.318(11)	Eu(4)−O(18)	2.314(13)
Eu(2)−O(19B)	2.383(11)	Eu(3)−O(13)	2.539(11)	Eu(4)−O(12B)	2.374(13)
Eu(2)−O(16B)	2.557(11)	Eu(3)−O(14B)	2.369(10)		
Eu(1)−Eu(3)	5.907(13)	Eu(4)−Eu(3)	5.827(12)	Eu(1)−Eu(6)	3.910(13)
Eu(2)−Eu(4)	6.146(10)	Eu(1)−Eu(4)	6.146(13)	Eu(4)−Eu(4)	6.536(12)
Eu(1)−Eu(8)	4.426(13)	Eu(4)−Eu(6)	6.557(12)	Eu(2)−Eu(3)	4.392(10)
		Compound **2**			
Eu(1)−O(1)	2.431(39)	Eu(1)−O(5A)	2.392(20)	Eu(1)−O(2A)	2.456(57)
Eu(1)−O(6)	2.369(23)	Eu(1)−O(3A)	2.362(21)	Eu(1)−O(34)	2.499(21)
Eu(1)−O(4A)	2.362(23)	Eu(1)−O(40)	2.407(21)	Al(1)−O(27)	2.871(30)
Eu(1)−Eu(1A)	6.288(88)				
		Compound **3**			
Eu(1)−O(1)	2.423(1)	Eu(1)−O(5)	2.362(5)	Eu(1)−O(2)	2.350(2)
Eu(1)−O(6)	2.346(2)	Eu(1)−O(3)	2.428(0)	Eu(1)−O(7)	2.421(3)
Eu(1)−O(4)	2.373(1)	Eu(1)−O(8)	2.380(1)		
		Compound **4**			
Eu(1)−O(1)	2.460(11)	Eu(1)−O(5)	2.419(10)	Eu(1)−O(2)	2.571(13)
Eu(1)−O(6)	2.437(13)	Eu(1)−O(3)	2.479(11)	Eu(1)−O(7)	2.447(11)
Eu(1)−O(4)	2.324(11)	Eu(1)−O(51A)	2.380(11)	Eu(1)−Eu(1A)	5.366(12)

the species observed in the case of Al(III) addition are $PW_{11}O_{39}^{7-}$ and $PW_{12}O_{40}^{3-}$.

Solution Speciation of $PW_9O_{34}^{9-}$ with Eu^{3+} After Mixing and Before Heating. The speciation reactions of $PW_9O_{34}^{9-}$ with Eu^{3+} involve adding the polyoxometalate to a solution containing Eu(III) at the appropriate pH and countercation content. The solutions are heated for 2 min at 90 °C; after this heating step, the ^{31}P NMR does not change over a period of days. Before the heating step, ^{31}P NMR analysis shows that there are unidentified, broad ^{31}P peaks that are likely due to chemical exchange processes of different species. For example, Figure S3 shows the ^{31}P NMR spectra for a typical reaction of $PW_9O_{34}^{9-}$ and Eu(III), 1:1 stoichiometry, pH ca. 6−7, before heating and after heating at 90 °C. Before heating, the spectrum is broad and the peak positions do not correspond to any of the identified species. However, it is apparent that the broad peaks represent dynamic behavior of species that are in chemical exchange. For example, the peak at 25.89 ppm is clearly the largest peak and likely represents an average of the peaks of species **1**, $\{(Eu_2PW_{10}O_{38})_4(W_3O_8)(H_2O)_2(OH)_4\}^{22-}$ (28.97, 22.55 ppm),[17] where the two chemically inequivalent ($Eu_2PW_{10}O_{38}$) lobes of the molecule are engaged in a dynamic process. The other peaks at 13.82 and 2.80 ppm are also broad and may represent chemical exchange as well. The peak at 2.80 ppm appears to be an average between species **2** and **3** $Eu(PW_{11}O_{39})^{4-}$ (5.28 ppm) and $Eu(PW_{11}O_{39})_2^{11-}$ (0.57 ppm) reflecting an exchange process involving these species. The peak at 13.82 ppm possibly represents exchange between all three species. Heating this solution results in clear conversion to species **1** (28.97, 22.55 ppm) and species **2** and **3**, ($Eu(PW_{11}O_{39})^{4-}$ (5.28 ppm) and $Eu(PW_{11}O_{39})_2^{11-}$ (0.57 ppm), respectively.

Conversion of the broad peaks (Figure S3) to species **1**−**3** also occurs if the solution is allowed to age for 12 h at room temperature. Aging experiments of the heated solutions show that the spectra do not change during a period of days, suggesting that the system has reached equilibrium.

Reaction of $PW_9O_{34}^{9-}$ with Eu^{3+} (1:1 Stoichiometry) at Different pH Values. The ^{31}P NMR spectra (Figure 1) for the reaction carried out at low pH (1−3) shows two peaks at 5.23 ppm and −11.93 ppm that correspond to species **2,** $Eu(PW_{11}O_{39})^{4-}$, and $PW_{11}O_{39}^{7-}$, respectively. Decomposition to $PW_{12}O_{40}^{3-}$ is also observed. Three species are observed at pH 7; these are **1**, $(Eu_2PW_{10}O_{38})_4(W_3O_8(H_2O)_2(OH)_4)^{22-}$ (δ, ppm: 28.55, 22.07), **2**, $Eu(PW_{11}O_{39})^{4-}$ (δ, ppm: 5.25 ppm), and **3**, $Eu(PW_{11}O_{39})_2^{11-}$ (δ, ppm: 0.5 ppm). The spectrum at pH 9 is dominated by species **1** and **3**.

The reaction of $PW_9O_{34}^{9-}$ with Eu^{3+} under varying pH values (4.5, 5.5, and 6.5) was examined in the presence of different cations (Li^+, Na^+, K^+) (Supporting Information, Figures S1 and S2). This experiment provides the opportunity to evaluate both the pH and counterion influence on speciation. With Li acetate or Na acetate buffer (0.5M) at pH 4.5 (Figure S1), the ^{31}P NMR of $PW_9O_{34}^{9-}$ and Eu^{3+} in a 1:1 mole ratio showed that **2** was the major solution species with the $PW_{11}O_{39}^{7-}$ ligand as a minor species. At pH 5.5, only species **2** was observed, while, at pH 6.5, two additional species **1** and **3** were present in the solution in low concentration.

Different behavior is observed with K^+ counterions (KOAc, 0.5 M). For example, at pH 4.5, the major species observed in solution are **2**, $Eu(PW_{11}O_{39})^{4-}$, and free $PW_{11}O_{39}^{7-}$, with **3**, $Eu(PW_{11}O_{39})_2^{11-}$, in significant concentration (Figure S2). Increasing the pH results in no observable free $PW_{11}O_{39}^{7-}$ and a significant increase in the concentration of species **3**. In contrast to the Li^+ and Na^+ case, species **3** grows in significantly at the lower pH values with K^+ as the buffer, until it is the dominant species at pH 7.6. Species **1** begins to appear at a higher pH of 7.6 compared to 6.5 found for the Li^+ and Na^+ buffers.

Expanded Study of $PW_9O_{34}^{9-}$ with Eu^{3+} (1:1 Stoichiometry) as a Function of Countercation. To further test the effect of countercations on speciation, a study of the speciation of $PW_9O_{34}^{9-}$ + Eu^{3+} (1:1 stoichiometry, pH 7) with an expanded series of countercations was carried out

(Figure 2). With Na^+ (not shown), K^+, or NH_4^+ (not shown), three species corresponding to **1** (28.8, 22.2 ppm), **2** (5.2 ppm), and **3** (0.5 ppm) can be identified, similar to studies reported above. Addition of Cs^+ into the aqueous solution of $PW_9O_{34}^{9-}$ + Eu^{3+} (1:1 stoichiometry, pH 7) results in exclusively one species, **3**, $Eu(PW_{11}O_{39})_2^{11-}$.

Solutions containing the countercation Al(III) show the presence of species **4** that has been identified as Eu(α-2-$P_2W_{17}O_{61})^{7-}$ by ^{31}P NMR and crystallography; vide infra.[14] This phenomenon was only seen in the presence of Al^{3+} and is possibly due to the acidity that Al^{3+} confers upon the solution; generally, the pH after treatment with $AlCl_3$ was ca. 2−3. Also, the ability of Al(III) to bind to oxygen atoms of polyoxometalates may influence the formation of this species. Species **2** and **3**, 1:1 $Eu(PW_{11}O_{39})^{4-}$ and 1:2 $Eu(PW_{11}O_{39})_2^{11-}$, respectively, are also found as the majority species in this solution (Figure 2).

The reaction of Eu(III) and A-$PW_9O_{34}^{9-}$ in H_2O, in both 1:1 or 2:1 Eu:A-$PW_9O_{34}^{9-}$ stoichiometry, with the addition of TBA^+ or TEA^+, resulted in isolation, by extraction into organic solution, of species **2**, $Eu(PW_{11}O_{39})^{4-}$, exclusively. The ^{31}P NMR of the TBA salt (δ, ppm, 5.3, H_2O; δ, ppm, 9.6, CH_3CN) was identical with that for a genuine sample of $TBA_3H\{EuPW_{11}O_{39}\}$ that was prepared directly by two methods (metathesis of the potassium salt of $Eu(PW_{11}O_{39})^{4-}$, prepared by direct reaction of Eu(III) and $PW_{11}O_{39}^{7-}$ or by reaction of $Eu(ClO_4)_3$ and $TBA_4H_3(PW_{11}O_{39})$[23] in CH_3CN). The samples of $TBA_3H\{EuPW_{11}O_{39}\}$ prepared directly have been analyzed by elemental analysis, thus far.

Reaction of $PW_9O_{34}^{9-}$ with Eu^{3+} under Different Stoichiometries. The reaction of Eu^{3+} and A-$PW_9O_{34}^{9-}$ in 0.5:1, 1:1, and 2:1 Eu: POM stoichiometric ratios were studied in NaOAc buffered solution (0.5 M, pH 6.5), and the ^{31}P NMR data are shown in Figure 3. ^{31}P NMR spectra show that at 0.5:1 Eu:$PW_9O_{34}^{9-}$ species **3**, $Eu(PW_{11}O_{39})_2^{11-}$, dominates while **2**, $Eu(PW_{11}O_{39})^{4-}$ and an unknown species at 1.99 ppm, possibly due to decomposition of PW_9^{9-} in solution,[24] are present in smaller quantities. At 1:1 Eu:$PW_9O_{34}^{9-}$ stoichiometry, three distinct species coexist in solution; according to ^{31}P NMR, these species are **1**, $\{(Eu_2PW_{10}O_{38})_4(W_3O_8(H_2O)_2(OH)_4\}^{22-}$, **2**, and **3**. At 2:1 Eu:$PW_9O_{34}^{9-}$, one species, **2**, is observed in the aqueous solution. The same speciation behavior is observed when the experiment is run in water, except that there are a few more small unidentified peaks in the 1:2 Eu:$PW_9O_{34}^{9-}$ sample, probably due to decomposition of PW_9^{9-} in solution.

Addition of $AlCl_3$ to solutions of 1:1 Eu:$PW_9O_{34}^{9-}$ stoichiometry resulted in the small amount $Eu(\alpha\text{-}2\text{-}P_2W_{17}O_{61})_2^{14-}$ (Figure 2). In contrast, upon addition of Al to 2:1 Eu:$PW_9O_{34}^{9-}$ stoichiometry, the $Eu(PW_{11}O_{39})^{4-}$ species was isolated as crystals in 45% yield; vide infra.

Isolation, Characterization of the Four Complexes Observed in Solution Speciation Studies, and Description of Crystal Structures. From careful analysis of the reactions reported above, we chose appropriate conditions to optimize the syntheses and isolate the four species **1**−**4** from reactions of $PW_9O_{34}^{9-}$ with Eu^{3+}. This is important to confidently identify the species and understand their formation. The procedures are summarized in Scheme 1.

Scheme 1. Synthetic Strategy for Isolation of Species **1**−**4** from Eu(III) and Isolation of $PW_9O_{34}^{9-}$

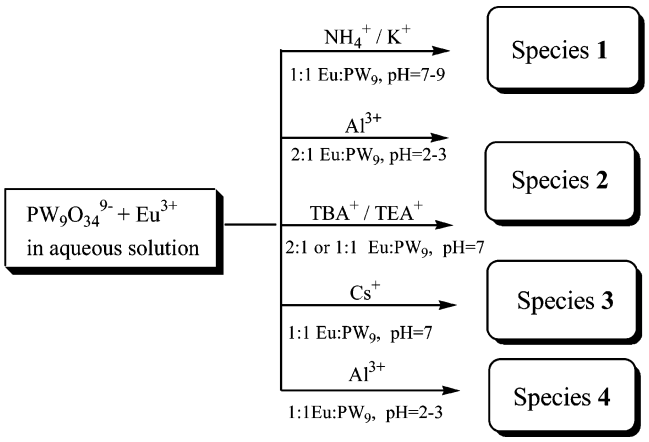

Table 3. Multinuclear NMR Data for **1**−**4**

compd	^{31}P NMR data (δ, ppm)
$[Eu_2PW_{10}O_{38})_4(W_3O_{14})]^{30-}$, **1**[a]	31.53, 23.22
$[Eu(H_2O)_xPW_{11}O_{39}]^{7-}$, **2**	5.25
$[Eu(PW_{11}O_{39})_2]^{11-}$, **3**	0.34
$[Eu(H_2O)_x(\alpha\text{-}2\text{-}P_2W_{17}O_{61})]^{14-}$, **4**	8.72, −12.23
$[Y(H_2O)_xPW_{11}O_{39}]^{7-}$	−12.04
$[Y(PW_{11}O_{39})_2]^{11-}$	−12.28

compd	^{183}W NMR data [δ, ppm (integration)]
$[Y_2PW_{10}O_{38})_4(W_3O_{14})]^{30-}$ [b]	−30.8 (2), −99.8 (2), −103.4 (2), −110.8 (2), −124.2 (2), −129.8 (2), −131.1 (2), −133.8 (2), −134.6 (2), −135.8 (2), −139.2 (2), −141.3 (1), −145.9 (2), −149.7 (2), −157.9 (2), −159.8 (2), −174.7 (2), −187.8 (2), −225.7 (2)
$[Y(H_2O)_xPW_{11}O_{39}]^{4-}$ [c]	−107.36 (2), −116.79 (1), −126.47 (2), −144.94 (2), −145.47 (2), −155.00 (2)
$[Eu(H_2O)_x(PW_{11}O_{39})]^{4-}$ [c]	−123.93 (1), −131.45 (2), −138.44 (2), −187.69 (2)
$[Y(PW_{11}O_{39})_2]^{11-}$ [c]	−130.00 (1), −132.02 (1), −143.93 (1), −149.42(1), −150.64 (1), −155.53 (1), −166.64 (1), −172.38 (1), 173.23 (1), −174.76 (1), −206.99 (1)

[a] Chemical shifts for crystalline sample of **1** in water. The chemical shifts for samples with high concentrations of counterions and other species are found slightly upfield at 28.55 and 22.07 ppm. [b] Howell, R. C.; Perez, F. G.; Jain, S.; Horrocks, W. D.; Rheingold, A. L.; Francesconi, L. C. *Angew. Chew., Int. Ed.* **2001**, *40* (21), 4031−4034. [c] The samples were prepared directly from $PW_{11}O_{39}^{7-}$ for ^{183}W NMR. The ^{31}P NMR for these samples was identical with samples prepared via $PW_9O_{34}^{9-}$.

Species 1. The addition of NH_4^+ at pH 7−9 to a solution of $PW_9O_{34}^{9-}$ and Eu^{3+} results in the isolation of **1** as chunky colorless rectangular blocks. The ^{31}P NMR chemical shifts (Table 3) for isolated crystalline samples of **1** are observed at 31.53 and 23.22 ppm and are dependent on solution conditions; in solution with different countercations present, the resonances are shifted upfield. We have reported the identical structure of the K^+ salts of Y(III) and Eu(III) analogues of **1**,[17] and therefore, complete structural details

(23) Ho, R. K. C.; Klemperer, W. G. *J. Am. Chem. Soc.* **1978**, *100*, 6772−6774.
(24) The peak at 1.99 ppm along with other small peaks were observed upon dissolving $PW_9O_{34}^{9-}$ alone in NaAc (0.5 M, pH 6.5, 30% D_2O).

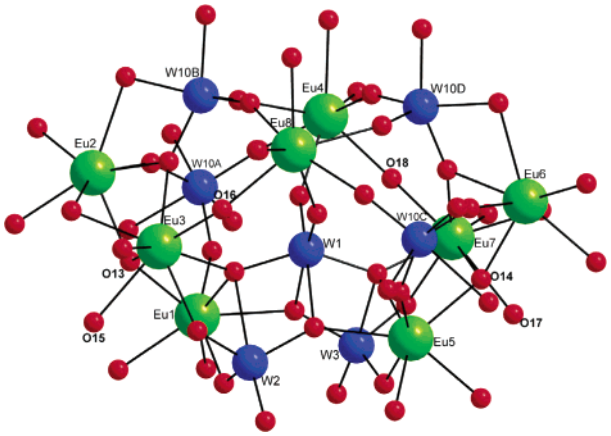

Figure 4. Structure of the central $W_8Eu_8(H_2O)_2(OH)_4O_{40}$ unit in $\{Eu_2PW_{10}O_{38})_4(W_3O_8(H_2O)_2(OH)_4)\}^{22-}$, **1**. Uncoordinated H_2O molecules have been removed for clarity (W, blue; O, red; Eu, green). Hydroxide and water oxygen atoms are labeled; see text.

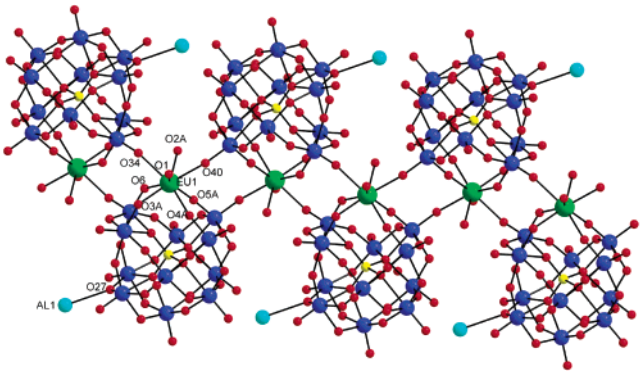

Figure 5. Ball and stick structure of $Al\{Eu(H_2O)_2(PW_{11}O_{39})\}^{-}$, **2**. Uncoordinated H_2O molecules have been removed for clarity. Legend: W, blue; O, red; Eu, green; P, yellow; Al, blue.

of the NH_4^+ salt are in the Supporting Information. Y(III) and Eu(III) also behave similarly with respect to solution speciation of $PW_9O_{34}^{9-}$, and thus, the Y(III) analogues are useful for solution characterization using ^{183}W NMR because resonances corresponding to all W atoms can be observed. The resonances corresponding to W atoms close to the site of substitution are often not observed in the Eu(III) analogues.

Species **1** forms easily with $PW_9O_{34}^{9-}$ at pH 6.5−9 in 76% yield and is uniquely stable in basic solution. From our previous work, multinuclear NMR and luminescence excitation spectra provide evidence that the cluster remains intact in aqueous solution, and the ^{31}P NMR data, provided in this study, show that the cluster remains intact under basic conditions and different countercation content. Increasing the acid content sets up an equilibrium with complex **2**, $Eu(PW_{11}O_{39})^{4-}$, that can be monitored by ^{31}P NMR, Figure S4. The Y(III) analogue shows the same equilibrium, and ^{183}W NMR of the Y(III) + $PW_9O_{34}^{9-}$ solution at pH 4.6 shows 6 peaks, of appropriate integration, that correspond to the 1:1 $Y(PW_{11}O_{39})^{4-}$ species, consistent with our assignment of $Eu(PW_{11}O_{39})^{4-}$.

1 can be viewed as the confluence of four $PW_{10}O_{37}^{9-}$ units each incorporating 2 Eu(III) ions to create four Keggin-like anions that are further tied together by three additional tungstate units, Figure S5.[17] The central core consists then of the eight Eu(III) ions coordinated to tungstate units, shown in Figure 4. Bond valence sums[25,26] (Table S3) performed on all of the oxygen atoms in this core suggest that four oxygen atoms, O13, O14, O16, and O18, each bridging two Eu(III) ions, are hydroxides and two oxygen atoms, O15 and O17, are water molecules bound to Eu(III) centers. This hydroxo/oxo core is expected given the neutral to basic pH required for the formation of this complex and the general Lewis acidity of the lanthanides.

Species 2. The addition of Al^{3+} into the solution of $PW_9O_{34}^{9-}$ with Eu^{3+} (2:1 Eu:POM) results in a drop in pH from 7 to 2.8. As the predominant polyoxotungstate species is the monovacant $PW_{11}O_{39}^{9-}$ at lower pH (Table S1), it is very reasonable that addition of Eu(III) will form $Eu(H_2O)_4PW_{11}O_{39}^{4-}$ especially in this case, with an excess of Eu(III). ^{31}P NMR and elemental analysis are consistent with this formulation.

As shown in Figure 5, in the solid-state, **2** is an infinite one-dimensional polymer, similar to the $Eu(H_2O)_2(SiW_{11}O_{39})^{5-}$ (K^+ salt) species published by Mialane recently.[4] The structure is similar also to $Ce(H_2O)_3(\alpha\text{-}SiW_{11}O_{39})^{5-}$ that also forms a one-dimensional polymer.[3] Due to the smaller size of Eu^{3+} than Ce^{3+}, it is reasonable that only two water molecules are coordinated to the Eu^{3+} rather than three water molecules that are found coordinated to Ce^{3+}. The Eu^{3+} is coordinated to four oxygen atoms of the defect site of $\alpha\text{-}PW_{11}O_{39}$, to two water molecules, and to two neighboring $\alpha\text{-}PW_{11}O_{39}$ units through terminal oxygen atoms. As observed for most lanthanide complexes of monovacant polyoxometalates, the Eu(III) ion is in a distorted monocapped square antiprism environment. The Al(III) ion sits in the space between the $\alpha\text{-}PW_{11}O_{39}$ units and shows a weak connection (average Al−O: 2.87(3) Å) to a terminal oxygen atom of an adjacent polyoxometalate. The structure contains 35.3% solvent accessible space.[27] Therefore, it is likely that water is located in this interstitial space as well.

The Eu(III)−O bond lengths to the four oxygen atoms in the Keggin defect are similar (average: 2.371 Å), and the average Eu(III)−oxygen bond lengths to the two neighboring $PW_{11}O_{39}$ moieties is longer at 2.453 Å. The Eu−$O(H_2O)$ distance is 2.455 Å within the range of Eu−$O(H_2O)$ bond distances.[4,14] The interatomic distances between the europium centers are 6.288 Å. The bond lengths for the atoms in the tungsten−oxygen framework of $Eu(H_2O)_2(PW_{11}O_{39})^{4-}$ compare favorably with other Keggin structures. Although **2** exists as an oligomer in the solid state, it is soluble in aqueous solution and the ^{31}P NMR is identical with a sample of $Eu(PW_{11}O_{39})^{4-}$, suggesting that the polymer dissociates into the monomeric form.

Species 3. Addition of Cs^+ to $PW_9O_{34}^{9-}$ and Eu^{3+} (1:1 stoichiometry) at pH 7 results in **3** as small colorless thick rectangular crystals. The crystal structure, Figure S6, shows that this species is a 1:2 Eu:$PW_{11}O_{39}^{7-}$ complex, originally

(25) Thorp, H. H. *Inorg. Chem.* **1992**, *31*, 1585−1588.
(26) Brown, I. D.; Altermatt, D. *Acta Crystallogr.* **1985**, *B41*, 244−247.
(27) Spek, A. L. *Acta Crystallogr.* **1990**, *A 46*, C34.

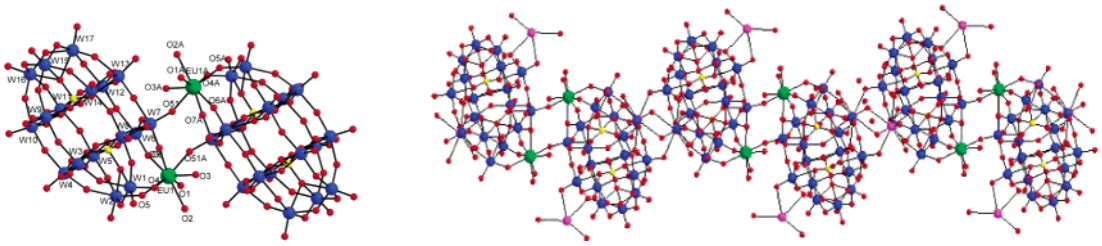

Figure 6. Left: Ball-and-stick structure of $\{Eu(H_2O)_3(\alpha\text{-}2\text{-}P_2W_{17}O_{61})\}_2^{14-}$, **4**. Right: Packing diagram of **4**, viewed along the *a* axis. Uncoordinated H_2O molecules have been removed for clarity. Legend: W, blue; O, red; Eu, green; P, yellow; Al, pink.

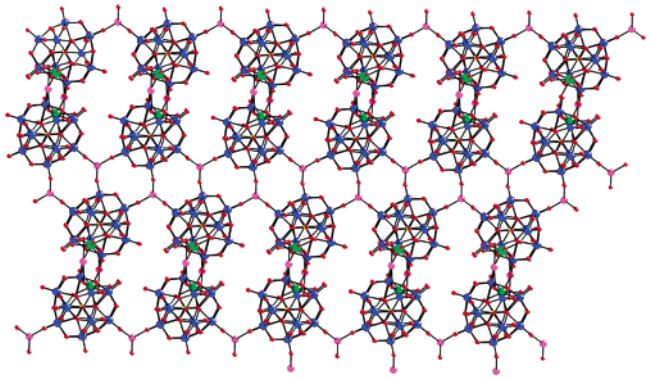

Figure 7. Packing diagram of **4**, viewed along the *c* axis. Uncoordinated H_2O molecules have been removed for clarity. Legend: W, blue; O, red; Eu, green; P, yellow; Al, pink.

isolated by Peacock and Weakley.[28] The ^{31}P NMR shows one peak at 0.34 ppm that is identical with the 1:2 Eu:$PW_{11}O_{39}^{7-}$ complex, prepared directly. The ^{183}W NMR of 1:2 analogue $Y(PW_{11}O_{39})_2^{11-}$ shows 11 peaks[11,29] (Table 3), consistent with the C_2 structure revealed by X-ray crystallography. All 11 Cs^+ ions were located and surround the $Eu(PW_{11}O_{39})_2^{11-}$ species (Figure S7), with 1 Cs^+ ion (C7) located in an interactive distance of 3.2 Å to both $PW_{11}O_{39}$ lobes.

Species 4. Addition of Al^{3+} into the solution of $PW_9O_{34}^{9-}$ + Eu^{3+} (1:1 stoichiometry) results in colorless chunky prisms of **4** in 53% yield. X-ray crystallography reveals the dimeric structure $\{Eu(H_2O)_3(\alpha\text{-}2\text{-}P_2W_{17}O_{61})\}_2^{14-}$ (Figure 6) that we have observed before from the reaction of excess Eu(III) with $\alpha\text{-}2\text{-}P_2W_{17}O_{61}^{10-}$ in a KCl medium.[14] However, in this case, the Al(III) serves as a counterion and forms weak connections with the terminal W−O bonds of adjacent $\{Eu(H_2O)_3(\alpha\text{-}2\text{-}P_2W_{17}O_{61})\}_2^{14-}$ units, seen in Figures 6 and 7.

The extended structure is composed of the anions of **4** linked together by surface bound Al^{3+} cations. The Al^{3+} ions, in a distorted trigonal prismatic coordination environment, bind to terminal oxygen atoms of two dimers (average Al−O distances: 2.77(5) Å) giving rise to chains along the crystallographic *a* axis (Figure 6), while, down the *c* axis, Al^{3+} links three $\{Eu(H_2O)_3(\alpha\text{-}2\text{-}P_2W_{17}O_{61}\}_2^{14-}$ units giving rise to the formation of discrete channels forming a porous 3D structure (pore size: 17 Å × 6 Å; Figure 7). This compound is less soluble in water than anions of similar size, probably due to the covalent bonding of the Eu^{3+} to a terminal oxygen of an adjacent polyoxoanion and to the surface bonding of the Al^{3+} cations. Both ^{31}P and ^{183}W NMR show good evidence to support the notion that the dimeric complex $\{Eu(H_2O)_3(\alpha\text{-}2\text{-}P_2W_{17}O_{61})\}_2^{14-}$ in the solid state dissociates in aqueous solution to form the monomeric form $Eu(\alpha\text{-}2\text{-}P_2W_{17}O_{61})^{7-}$ (Table 3).

Discussion

Three parameters, pH, countercation, and stoichiometry, have an important impact on the aqueous speciation of $PW_9O_{34}^{9-}$ and Eu^{3+}. The pH influences the speciation of the polyoxometalate $PW_9O_{34}^{9-}$, alone, to form primarily $PW_{11}O_{39}^{7-}$ ligand[22] and decomposition products (Table S1) to which the Eu(III) can bind. The countercations modulate the reactivity and may be instrumental in anchoring polyoxometalate units together for assembling larger structures, such as the "sandwich" complex $Eu(PW_{11}O_{39})_2^{11-}$, **3**, and the hydroxo/oxo cluster, **1**.[30]

Under low pH conditions, the high acid content stabilizes the $PW_{11}O_{39}^{7-}$ ligand as well as species **2**, $Eu(PW_{11}O_{39})^{4-}$, the 1:1 species. As the base is increased, and proton competition with the $PW_{11}O_{39}^{7-}$ ligand and $Eu(PW_{11}O_{39})^{4-}$ (**2**) decreases, the concentration of the 1:2 complex, $Eu(PW_{11}O_{39})_2^{11-}$ (**3**), is increased. Eventually at high pH, where $PW_9O_{34}^{9-}$ decomposes to $PW_{11}O_{39}^{7-}$, lower nuclearity phosphotungstates, as well as WO_4^{2-} species **3** and **1**, become major components of the solution, as seen in Figures 1, S1, and S2. Species **1** is comprised of the $PW_{10}O_{38}^{11-}$ fragment and monotungstate units bound to Eu(III).

Cations have a significant effect on the speciation of $PW_9O_{34}^{9-}$ and Eu(III). The hypothesis that large, less extensively hydrated alkali metal cations bind to the surfaces of the polyoxometalates and "anchor" the POM units in place for assembly into larger structures, such as the 1:2 sandwich structures, has been put forward.[31,32] Ion pairing of large cations (Rb^+) to POM surfaces was proposed by Kirby and Baker in a study to understand the solution "syn" structure of $Th(\alpha\text{-}2\text{-}P_2W_{17}O_{61})_2$.[16−31] The formation of a 1:2 K^+:$SiW_{11}O_{39}$ species in a Cs^+ environment has been reported recently by Laronze.[32] In this latter study, similar to ours, treatment of the trivacant A-α-$SiW_9O_{34}^{10-}$ with K^+ and

(28) Peacock, R. D.; Weakley, T. J. R. *J. Chem. Soc.* **1971**, *A*, 1836−39.
(29) Fedotov, M. A.; Pertsikov, B. Z.; Danovich, D. K. *Polyhedron* **1990**, *9*, 1249−1256.
(30) We have also observed Eu(III) and Eu(III)−OH−Eu(III) dimeric units serving as countercations. These moieties bind to terminal W=O bonds of polyoxometalates: Zhang, C.; Howell, R. C.; Francesconi, L. C. Manuscript in preparation, 2004.
(31) Kirby, J. F.; Baker, L., C. W. *Inorg. Chem.* **1998**, *37*, 5537−5545.
(32) Laronze, N.; Marrot, J.; Herve, G. *Inorg. Chem.* **2003**, *42*, 5857−5862.

excess Cs^+ results in isolation of $Cs_{15}K(SiW_{11}O_{39})_2$, where K^+ is bound in the cavity. This molecule is similar to **3**, with cubic coordination about the K^+ rather than square antiprismatic coordination geometry that is prevalent with the lanthanides. They propose, according to the solid-state crystal structure, that the Cs^+ anchors the $SiW_{11}O_{39}^{8-}$ species in place for the formation of the 1:2 K^+:POM complex. To substantiate this proposal, the solid-state structure of $Cs_{15}K(SiW_{11}O_{39})_2$ shows that three Cs^+ ions are bound to terminal oxygen atoms of each $SiW_{11}O_{39}^{10-}$ unit (with Cs−O distances of ca. 3.2 Å) perhaps stabilizing the $K(SiW_{11}O_{39})_2^{15-}$ solid-state structure. The molecule dissociates in aqueous solution.

Similarly, we have observed that in aqueous solution K^+ and Cs^+ promote the formation of the 1:2 $Eu(PW_{11}O_{39})_2^{11-}$ species. The formation of species **3**, 1:2 $Eu(PW_{11}O_{39})_2^{11-}$, in significant concentration is observed at low pH (4.5) for solutions containing K^+ buffer (Figure S2). In contrast **3** appears only at higher pH (6.5) with Li^+- and Na^+-containing buffers and in very low quantities (Figures 2 and S1). When Cs^+ is employed as a counterion, **3** is the only species formed (Figure 2). These observations are consistent with ion pairing of K^+ and Cs^+ to the $PW_{11}O_{39}$ lobes, thus anchoring the $PW_{11}O_{39}$ lobes in position to form the 1:2 complex.

Considering the solid-state structure of $Cs_{11}Eu(PW_{11}O_{39})_2$, one Cs^+ (Cs7) is in close contact with the terminal W−O and bridging W−O oxygen atoms (3.2 Å) from both lobes and may be a prototype as to the role large cations have in stabilizing this structure. The remaining 10 Cs^+ ions surround the sandwich complex. The Cs^+ ions may insulate and stabilize the sandwich $Eu(PW_{11}O_{39})_2$ ions in the crystal. Similar interaction of Cs^+ ions with the metal oxygen surfaces may stabilize this structure in solution as well.

Ion pairing of alkali metal cations to polyoxometalates has been quantitated in recent studies. The larger and less extensively solvated alkali-metal cations form smaller (more intimate) association complexes with the $\{X^{n+}VW_{11}O_{40}\}^{(9-n)-}$ (X = P(V), Si(IV), Al(III)) family of polyoxometalates.[33,34] The smaller association complexes impact physical properties of the polyoxometalates, for example the diffusion coefficients and electron-transfer rates of organic oxidation reactions. The countercation effect can be further substantiated by our observations on the solution speciation of the 1:2 Ln-$(\alpha\text{-}1\text{-}P_2W_{17}O_{61})_2^{14-}$ species.[35] We find that countercations are critical to the formation of 1:2 $Ln(\alpha\text{-}1\text{-}P_2W_{17}O_{61})_2^{14-}$ species in aqueous solution. In these studies, ^{31}P NMR shows clearly that in aqueous solution the 1:2 species is maintained in Cs^+ buffer, whereas an equilibrium between the 1:1 and 1:2 is set up with K^+. Li^+ buffer results in complete dissociation of the 1:2 $Ln(\alpha\text{-}1\text{-}P_2W_{17}O_{61})_2^{14-}$ species into the 1:1 $Ln(\alpha\text{-}1\text{-}P_2W_{17}O_{61})^{7-}$ species and $(\alpha\text{-}1\text{-}P_2W_{17}O_{61})^{10-}$ ligand. We suspect that the Cs^+ ions and, to an extent, the K^+ ions are binding to surface sites of POMs and thus stabilize the 1:2 structures in solution.

In contrast, the addition of large organic counterions such as tetrabutylammonium (TBA^+) chloride or tetraethylammonium (TEA^+) chloride into the solution of $PW_9O_{34}^{9-}$ + Eu^{3+} (2:1 and 1:1 Eu:$PW_9O_{34}^{9-}$ stoichiometry) results in formation of exclusively species **2**, $Eu(PW_{11}O_{39})^{4-}$. It has been demonstrated recently, in ion-pairing experiments, that large organic countercations do not bind to the surface of POMs to form ion pairs.[34] The stabilization of the 1:1 $Eu(PW_{11}O_{39})^{4-}$ over the 1:2 $Eu(PW_{11}O_{39})_2^{11-}$ species with TBA and TEA, then, is consistent with their lack of binding to the POM surfaces.

The effect of Al(III) as a counterion has also been probed. To understand the formation of the $Eu(\alpha\text{-}2\text{-}P_2W_{17}O_{61})_2^{14-}$ species, **4**, with the addition of Al(III), we analyzed solutions of the $PW_9O_{34}^{9-}$ ligand in the presence of Al^{3+}. Treatment of $PW_9O_{34}^{9-}$ with Al(III) results in a lowering of the pH to 2−3, and it is possible that condensation of two α-A-$PW_9O_{34}^{9-}$ moieties can occur. The ^{31}P NMR reveals small, equal-intensity peaks that likely correspond to a Wells−Dawson molecule, possibly a β-$P_2W_{18}O_{62}$ molecule, an α-$P_2W_{18}O_{62}$ with Al(III) bonded unsymmetrically to its faces, or the monolacunary $\alpha2\text{-}P_2W_{17}O_{61}^{10-}$ with Al(III) occupying the vacancy or near the vacancy (Table S1). It is likely that Eu(III) binds into the vacancy to form the small amount of complex **4** observed in the solution (Figure 2).

The stoichiometry of Eu and $PW_9O_{34}^{9-}$ play an important role in the speciation of Eu polyoxometalates, as shown in Figure 3. In an excess of $PW_9O_{34}^{9-}$ at pH 7, decomposition to primarily $PW_{11}O_{39}^{7-}$ with some unidentified P-containing products and phosphate as well as tungstate (Table S1) results in formation of both $Eu(PW_{11}O_{39})_2^{11-}$, **3**, and $Eu(PW_{11}O_{39})^{4-}$, **2**. With more Eu(III) present, as in 1:1 stoichiometry, under neutral conditions and with Na^+, K^+, and NH_4^+, $PW_{11}O_{39}^{7-}$ and lower nuclearity phosphotungstates (such as $PW_{10}O_{38}^{11-}$) can be trapped by the excess Eu(III) ions and monotungstate groups to form Eu_8 hydroxo/oxo cluster **1**. The 2:1 Eu:$PW_9O_{34}^{9-}$ stoichiometry provides an excess of Eu(III) ions to promote formation of $Eu(PW_{11}O_{39})^{4-}$, **2**.

The crystal structures of species **2** and **4**, shown in Figures 5−7, are instructive to examine the potential interaction of oxophilic Al(III) counterions with polyoxometalate surfaces. Species **2** and **4** show weak interactions of the Al(III) ions with terminal oxygen atoms of the polyoxometalate. The interaction, although weak, allows connection of the polyoxometalates and buildup of a porous material, as seen in species **4**.

We have investigated only the effects of pH and countercation in this study. However, other ions also can serve as templates or structure-directing groups. This was seen clearly in a recent report by Hill wherein the addition of carbonate to an aqueous solution of $Y^{III}Cl_3$ followed by addition of $Na_8HA\text{-}\alpha\text{-}PW_9O_{34}$ and workup forms 33% of a new complex that consists of a $Y_3(PW_9O_{34})_2$ sandwich complex wherein CO_3^{2-} anchors the Y(III) ions and the two POM units.[36] We find that species **1** forms without the addition of CO_3^{2-}. In this case, carbonate appears to template

(33) Grigoriev, V. A.; Hill, C. L.; Weinstock, I. A. *J. Am. Chem. Soc.* **2000**, *122*, 3544−3545.
(34) Grigoriev, V. A.; Cheng, D.; Hill, C. L.; Weinstock, I. A. *J. Am. Chem. Soc.* **2001**, *123*, 5292−5307.
(35) Cheng, Z.; Howell, R. C.; Luo, Q.; Fieselmann, H. L.; Todaro, L.; Francesconi, L. C. **2004**, manuscript in preparation.

the formation of this sandwich complex. The structure is reminiscent of the $Cu_3(PW_9O_{34})_2$ templated by nitrate anion.[37]

We employ multinuclear NMR coupled with X-ray crystallography in these studies; these techniques allow us to understand the speciation unambiguously. We and others have also used luminescence of Eu(III) for the study of speciation of lanthanide polyoxometalates.[4,12,14,17] Eu(III) luminescence is very informative to identify the number of species in solution, the coordination environment, and the number of bound water molecules. Luminescence studies (excitation, emission spectra, and luminescence lifetimes) of the 1:1 and 1:2 Eu:$(PW_{11}O_{39})^{7-}$ species have been reported.[38−41] These studies show that the 1:1 species has four bound water molecules, while the 1:2 species is not bound to water molecules. These are consistent with our structural and solution data, reported herein.

Conclusion

We have focused this study on understanding speciation chemistry of lanthanide complexes of the trivacant polyoxometalate $PW_9O_{34}^{9-}$ in aqueous solution. The A-α-$PW_9O_{34}^{9-}$ has 6 basic oxygen atoms that are available for bonding. The reaction products are highly dependent on the pH, countercation, and stoichiometry between Eu(III) and $PW_9O_{34}^{9-}$. The four species that have been observed in solution speciation studies have been synthesized and thoroughly characterized in the solid state and in solution. The pH has a profound effect on the speciation; at low pH, $(PW_{11}O_{39})^{7-}$ predominates and the 1:1 Eu$(PW_{11}O_{39})^{4-}$, **2**, forms. As the pH is increased, the 1:2 Weakley complex, Eu$(PW_{11}O_{39})_2^{11-}$ species, **3**, and a Eu_8 hydroxo/oxo cluster, **1**, forms. The countercations modulate this effect. Large countercations, such as K^+ and Cs^+, with low hydrodynamic radii (compared to Li^+ and Na^+) promote the formation of 1:2 Eu$(PW_{11}O_{39})^{4-}$ species, **3**, and **1**, at low pH values. We postulate that these large countercations can interact with the polyoxometalate surface and position one Eu$(PW_{11}O_{39})^{4-}$ unit for binding by a second $(PW_{11}O_{39})^{7-}$ moiety. The formation of $\{Eu(H_2O)_3(\alpha\text{-}2\text{-}P_2W_{17}O_{61})\}_2$, **4**, with Al(III) ions bound to terminal W−O bonds is observed when Al(III) is employed as a countercation.

Acknowledgment. We acknowledge the following sources of support for this research: NIH MARC/MBRS program (F.G.P., K.B.S.); Gertrude Elion Fellowship and Rose Kfar Rose Dissertation Award (C.Z.); Faculty Research Award Program of the City University of New York, National Science Foundation Grant No. CHE-0414218, Grant NIH-S06 GM60654 (SCORE) (L.C.F.); NSF Grant MRI0116244 for the purchase of an X-ray Diffractometer. Research infrastructure at Hunter College is partially supported by NIH-Research Centers in Minority Institutions Grant RR03037-08.

Supporting Information Available: Tables S1 and S2; ^{31}P NMR chemical shifts for speciation of $PW_9O_{34}^{9-}$ as a function of pH, buffer, and countercation and bond valence sum calculations; Figures S1−S7; and CIF files for the X-ray crystal structures of species **1**−**4**. This material is available free of charge via the Internet at http://pubs.acs.org.

IC049655H

(36) Fang, X.; Anderson, T. M.; Neiwert, W. A.; Hill, C. L. *Inorg. Chem.* **2003**, *42*, 8600−8602.
(37) Knoth, W. H.; Domaille, P. J.; Harlow, R. L. *Inorg. Chem.* **1986**, *25*, 1577−1584.
(38) Lis, S.; But, S. *J. Alloys Compd.* **2000**, *300*−*301*, 370−376.
(39) Yusov, A. B.; Fedoseev, A. M. *Radiokhimiya* **1992**, *34*, 61−70.
(40) Blasse, G.; Dirksen, G. J.; Zonnevijlle, F. *J. Inorg. Nucl. Chem.* **1981**, *43*, 2847−2853.
(41) Van Pelt, C. E.; Crooks, W. J., III.; Choppin, G. R. *Inorg. Chim. Acta* **2003**, in press.